Optimization of Titanium Dioxide Nanoparticles in Mesoporous Electron Transport Layer Perovskite Solar Cell

Deborah Augustine [a],*, Erlyta Septa Rosa [b], Niki Prastomo [c], Shobih [b]

[a]*Department of Physics Energy Engineering*
Surya University
F8 & F9 Grand Serpong Mall, Jl. MH Thamrin Panuggangan Utara, Pinang
Tangerang, Indonesia
[b]*Research Center for Electronics and Telecommunication*
Indonesia Institute of Sciences (P2ET-LIPI)
Komplek LIPI Gedung 20 Lt.4, Jl. Sangkuriang Cisitu
Bandung, Indonesia
[c]*Department of Physics Engineering*
Universitas Multimedia Nusantara
Jl. Scientia Boulevard, Gading Serpong
Tangerang, Indonesia

Abstract

Research about mesoporous TiO_2 as an electron transport layer in perovskite solar cell has been done to obtain the best fabricated cell's performance. In this research, the concentrations of opaque and transparent TiO_2 nanoparticle were varied, in order to optimize the TiO_2 mesoporous electron transport layer in FTO/CL-TiO_2/MS-TiO_2/Perovskite/P3HT/Ag perovskite-based solar cell. Morphological, optical, and electrical characteristics of TiO_2 layers were investigated using scanning electron microscopy (SEM), four-point probe (FPP), and UV-Vis spectroscopy. The influences of those characteristics in solar cell performance were analyzed by using illumination of sun simulator with a light intensity of 500 W/m^2. The results showed that transparent TiO_2 has a higher conductivity and transmittance compared to the opaque TiO_2. The concentration of TiO_2 solution in 1:17 ratio resulted in higher electrical performance in both the transparent and opaque TiO_2 layer. The best perovskite solar cell performance with PCE of 0.37% was achieved from the sample using TiO_2 transparent layer with a concentration of 1:7 ratio.

Keywords: mesoporous TiO_2, electron transport layer, perovskite solar cell.

I. INTRODUCTION

Perovskite solar cell (PSC) is one of the 3rd generation solar cells that has a simpler and low-cost fabrication [1]. Organometal halide, specifically leads methyl ammonium triiodide ($CH_3NH_3PbI_3$) has a perovskite structure, which can be used as an active light-absorbing layer because of its direct bandgap, a large absorption coefficient, good electron and hole conductivity, and high charge carrier mobility [2,3].

Typical device architectures of PSC consist of thin layers of transparent conductive oxide (TCO), electron-transporting layer (ETL), perovskite light-absorber layer, hole transport layer (HTL), and a metal electrode [4]. Depending on the sequence of depositing the ETL and HTL, the device structure can be divided into conventional versus inverted architectures. The order and chemical nature of the layers and the metal electrode strongly condition the performance of PSC [5].

The electron-transporting layer plays a crucial part in the PSC because it prevents the carriers from directly contacting the conductive substrate and thereby shunting the device. Inorganic semiconductors such as titanium dioxide (TiO_2) and zinc oxide (ZnO) are often used as an electron transport layer in PSC. Organic materials such as PCBM, C60, and their derivatives can also be used with inverted architecture [6]-[8].

Titanium dioxide is the most common material used because it has a suitable fermi level with lead methyl ammonium triiodide or MAI ($CH_3NH_3PbI_3$) perovskite, so that electron could easily be injected into its conductive band [9]. Relatively stable, long electron lifetime and simple fabrication methods are also the factors why TiO_2 is selected as an electron transport material [10]. Spin coating (SC) and spray pyrolysis (SP) are two representative solution processes used to form TiO_2 ETL, although atomic layer deposition (ALD), thermal oxidation, $TiCl_4$ chemical bath deposition, and screen printing have also been reported in the literature [11]. It is generally acknowledged that the quality of ETL produced is highly sensitive to process parameters, and thus the efficiency and reproducibility can vary substantially. The quality of the ETL can be improved by controlling both layer thickness and morphology. ETL thickness is very influential on the ease of electrons to flow to the anode and the optical properties of cells [12]. Mesoporous

structure of the ETL surface can lead perovskite to enter the pores and causes a larger surface area of the perovskite layer [13]. Although the properties of the TiO_2 layer in solid-state PSCs have been widely investigated, thickness- and morphology-dependent effects of the mesoscopic TiO_2 layer are still unclear. Therefore, in this study, these parameters will be investigated to obtain the optimum ETL TiO_2 layer in the process of making perovskite solar cells. The TiO_2 material used in this research is transparent and opaque TiO_2 pastes. The transparent paste contains a uniform of 20 nm TiO_2 particles, while opaque TiO_2 paste contains a mixture of 20 nm and 450 nm TiO_2 particles. In this research, the TiO_2 layers were deposited by a spin coating method, and because of the material used is in the form of a paste, it is necessary to dilute the pastes to make it possible to do the spin coating process. The concentration of the TiO_2 solution was varied by diluting TiO_2 pastes in ethanol, with a mass ratio of 1:3, 1:5, 1:7, 1:9, and 1:11, respectively.

II. EXPERIMENTAL SECTION

A. Materials

The substrate used in this research is fluorine-doped tin oxide (FTO) glass coated with a sheet resistivity of ~15 Ω/sq (Dyesol, TEC15). TiO_2 opaque (18NR-AO) and transparent (18NR-T) pastes were also purchased from Dyesol. $TiCl_4$ synthetic grade was obtained from Merck, while CH_3NH_3I (MAI), PbI_2, DMF, chlorobenzene, isopropyl alcohol, and silver wire were ordered from Sigma Aldrich as a pure analyzed grade.

B. Procedure

FTO glass substrates with the size of 2 cm × 1.5 cm were sonicated in Teepol, deionized (DI) water, and isopropyl alcohol (IPA) for 10 minutes, respectively. After being dried in the air, the substrates were immersed in 40 mM $TiCl_4$ solution at 70°C for 30 minutes, then they were rinsed with Deionized (DI) water and then annealed at 500°C for 30 minutes in the furnace to form TiO_2 compact layer.

TABLE 1
RESEARCH SAMPLE MAPPING

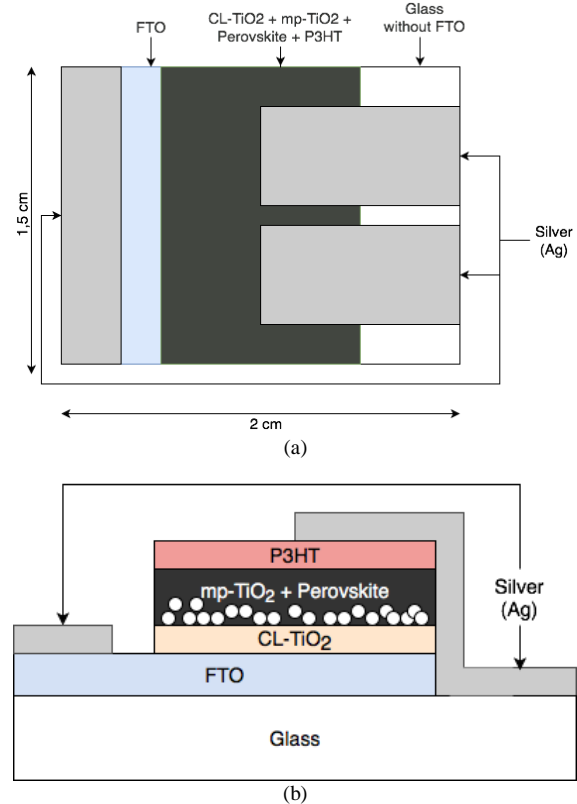| No	Sample Name	Type of TiO₂	Particle Size (nm)	TiO₂ : Ethanol Ratio (w/w)
1	1:3 T			1:3
2	1:5 T			1:5
3	1:7 T	18NR-T (Transparent)	20	1:7
4	1:9 T			1:9
5	1:11 T			1:11
6	1:3 AO			1:3
7	1:5 AO			1:5
8	1:7 AO	18NR-AO (Opaque)	20 – 450	1:7
9	1:9 AO			1:9
10	1:11 AO			1:11

Figure 1. Device Structure: (a) Top view, (b) Side view.

In this study, we use two types of TiO_2 pastes, which are commercially available. The opaque TiO_2 paste contains a mixture of 20 nm and 450 nm TiO_2 nanoparticles; meanwhile, the transparent one contains a uniform of 20 nm nanoparticles. Both of these pastes have very high viscosity. The spin coating technique used in this study requires materials with low viscosity. Therefore, the two pastes need to be diluted first. The TiO_2 pastes were diluted in ethanol as a dispersant. Since the paste has a very high viscosity, it is more convenient to prepare the samples with mass ratio, not volume ratio [14]. The concentration was varied in the mass ratio of 1:3, 1:5, 1:7, 1:9, and 1:11, respectively. Table 1 shows the name of samples, type of paste, and the ratio between TiO_2 and ethanol, which were used.

A 75 μl of the TiO_2 solution was spin-coated on the substrates at 5000 rpm for 30 seconds and dried at 70°C for 10 minutes in the oven, before annealing the substrates in the furnace at 500 °C for 30 minutes. $MAPbI_3$ perovskite solution was prepared by mixing MAI and PbI_2 in a molar ratio of 1:1 in DMF, resulting in a concentration of 35 wt%. The solution was stirred overnight at 65°C in order to dissolve it uniformly. A 75 μl perovskite solution was spin-coated at 4500 rpm for 30 seconds. At 4th second in the spin-coating process, 150 μl of chlorobenzene as anti-dispersant was dropped onto the spinning substrate. The perovskite layers were annealed on a hotplate at 95°C for 30 minutes.

A solution of 15 mg poly-3hexylthiopene (P3HT) in 1 ml chlorobenzene was prepared as HTL. The solution was stirred for 2 hours and then spin-coated on the surface of the perovskite layer at 3000 rpm for 30 seconds. The substrates were annealed on the hotplate at

95°C for 10 minutes. Finally, a 70 nm-thick silver electrode was deposited by thermal evaporation onto P3HT layer at a vacuum pressure of 5×10^{-5} mBar. The device structure can be seen in Figure 1.

C. Characterization

The morphology characteristics of the mesoporous TiO_2 layer were observed using a 20 kV scanning electron microscopy (SEM) JEOL JSM IT-300. The layer thickness was also obtained using the scaled cross-section images that had been generated by SEM. Meanwhile, the transmittance spectra of the electron transport layer were obtained with an ultraviolet spectrophotometer (Hewlett Packard 8453 Agilent Technologies). The sheet resistance of the TiO_2 layers was measured by a four-point probe using an HP 3468A electrometer. The photovoltaic performance of the fabricated perovskite solar cells was measured by the National Instrument I-V measurement system using sun simulator (Oriel, Newport, USA, AM1.5G) with the intensity of 500 W/m^2.

III. RESULTS AND DISCUSSION

The configuration of the device was FTO/CL-TiO_2/MS-TiO_2/Perovskite/P3HT/Ag. Band-alignment of anode, electron transport layer (TiO_2), light-absorbing layer (perovskite), hole transport layer (P3HT), and the cathode (Ag) is shown in Figure 2. This energy-level diagram could also be used to calculate open-circuit voltage (V_{oc}) in theory, which is the difference between lowest unoccupied molecular orbital (LUMO) energy or conduction band in the electron transport layer and highest occupied molecular orbital (HOMO) or valence band in hole transport layer [15]. LUMO of TiO_2 is -4.1 eV; meanwhile, HOMO of P3HT is -5.2 eV. By definition, the value of V_{oc}, in theory, is LUMO (TiO_2) – HOMO (P3HT), which is -4.1 eV – (-5.2 eV) or 1.1 eV.

SEM images of the surface morphology of opaque and transparent TiO_2 mesoporous layer in different concentrations were shown in Figure 3. It was observed in the figure that random large particles are present between fine particles on the opaque TiO_2 layer.
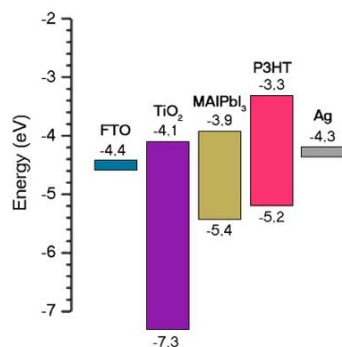
Figure 2. Schematic energy-level diagram for layers in the fabricated perovskite solar cell.
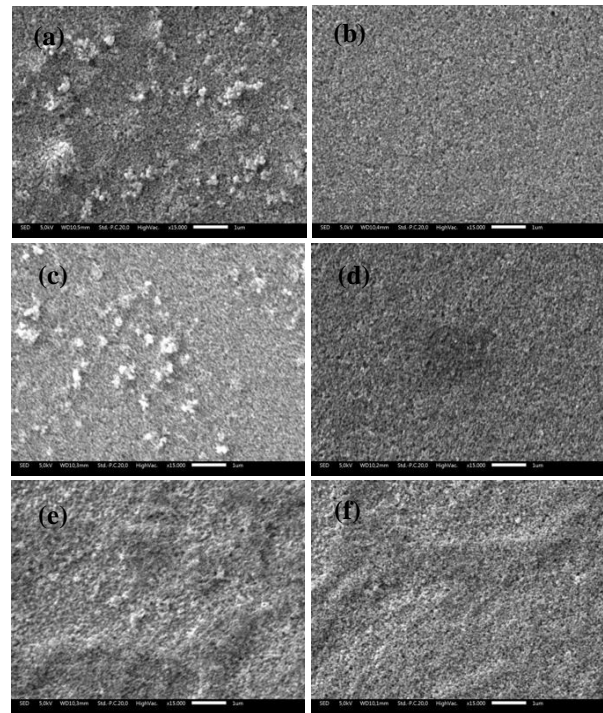
Figure 3. SEM images of TiO_2 ETL surface: (a) 1:3 AO, (b) 1:3 T, (c) 1:7 AO, (d) 1:7 T, (e) 1:11 AO, and (f) 1:11 T.

The number of large particles decreases with decreasing concentration of TiO_2 paste, so the surface tends to be smoother. Different from the opaque TiO_2 layer, in a transparent TiO_2 layer, the layer produces a uniform surface with evenly distributed particle size. The surface becomes increasingly uneven with decreasing concentration. It also shows the formation of contours with decreased concentration, both on the opaque and transparent TiO_2 layer.

The thickness of the TiO_2 layers was measured from the SEM image of the cross-section side of the samples (Figure 4). Figure 5 shows the thickness of the transparent and opaque TiO_2 layer under different concentration (ratio). Each samples' thickness was measured in three different points, and by those thickness data, error bars in Figure 5 were calculated. It was observed that increasing TiO_2 concentration in the solution would thicken the deposited layer for both opaque and transparent pastes. This observation verifies that TiO_2 mesoporous structure's thickness could be adjusted by varying TiO_2 concentrations in the solution or by arranging the ratio of TiO_2 paste and ethanol. Figure 5 also shows that opaque TiO_2 produces a thicker layer than the transparent one. The result from the TiO_2 opaque device is thicker than the device with the TiO_2 transparent layer because it has some broader particle sizes, either smaller or bigger particles (20 nm and 450 nm). While the device with the TiO_2 transparent layer a uniform particle size around 20 nm. Ito et al. also found that the TiO_2 layer would thicken as its particle was increasing in size without changing its solution volume in the deposition process [16].
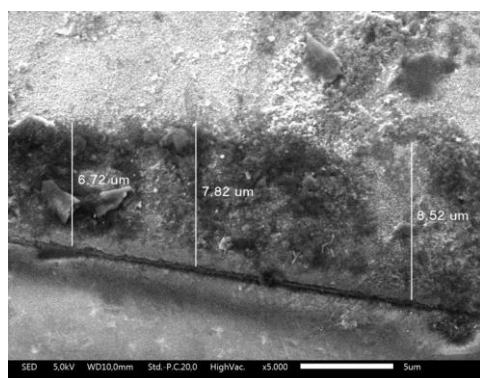
Figure 4. Thickness measurement of the TiO_2 layer by SEM image through the cross-section side of the TiO_2 layer.
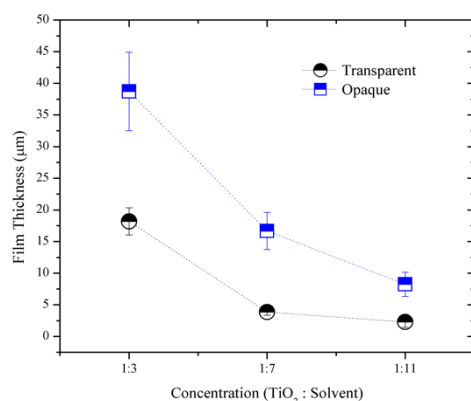

Figure 5. Thickness of TiO_2 mesoporous electron transport layer of different type of TiO_2 paste under different concentration

The thickness of a TiO_2 layer could affect the electron-hole recombination rate in the perovskite solar cell [13]. A thinner electron transport layer would have a shorter electron travel distance and reduce the cell's recombination rate. However, a thinner layer would reduce the deposited perovskite volume on it because of its mesoporous structure that acts as a scaffold for the perovskite layer [14].

An optical characteristic of the TiO_2 layer can be seen in Figure 6. As the name suggests, TiO_2 opaque produces an opaque layer, and on the other hand, TiO_2 transparent produces a transparent layer. Thus, the TiO_2 transparent layer was able to transmit light better than the TiO_2 opaque layer, as seen in the transmittance curve in Figure 6. Both TiO_2 transparent and opaque have a high transmittance in the visible region (400 – 800 nm), but in the ultraviolet region (400 nm) has a low transmittance. These optical properties are due to optical properties of TiO_2 nanoparticle itself that is able to absorb ultraviolet because of its wide bandgap of 3.0 eV – 3.2 eV [10].

From Figure 6(a), we can see that substrate with TiO_2 transparent did not have any significant difference between ratios of TiO_2 and ethanol. The highest transmittance of 93% is obtained by sample 1:9 T, while sample 1:7 T has the lowest transmittance value of 75%. In theory, sample 1:11 T should have the highest transmittance value. However, that position was obtained by sample 1:9 T. This could be caused by the uneven surface contour of sample 1:11, as seen in

Figure 3(f). When light meets an object with an uneven surface, it will be scattered. Hence it reduces the transmitted light [14].

On the other hand, samples with TiO_2 opaque have a significant difference between each concentration ratio value, as can be seen in Figure 6(b). Mainly in ratio 1:3 and 1:11, where the value is 4% and 74% respectively in wavelength of ~480 nm. It was shown that the transmittance is decreasing with increasing TiO_2 concentration. One of the possible causes is the increase of the layer thickness as TiO_2 concentration increases. When the layer thickens, the transparency of a layer will be reduced, and thus, transmittance value becomes less because the light will be absorbed by the addition layer [17].

As seen in Figure 6a and b, the control sample has a lower transmittance value than all transparent paste samples and opaque paste with a concentration of 1:9 and 1:11. This result is caused by the difference of TiO_2 material used in the deposition process. In the control sample, TiO_2 compact layer is deposited by the chemical bath method using $TiCl_4$ as the base material, whereas in other samples, TiO_2 is deposited by spin-coating using commercially available TiO_2 paste that has nano-sized particle and more even particle size distribution.
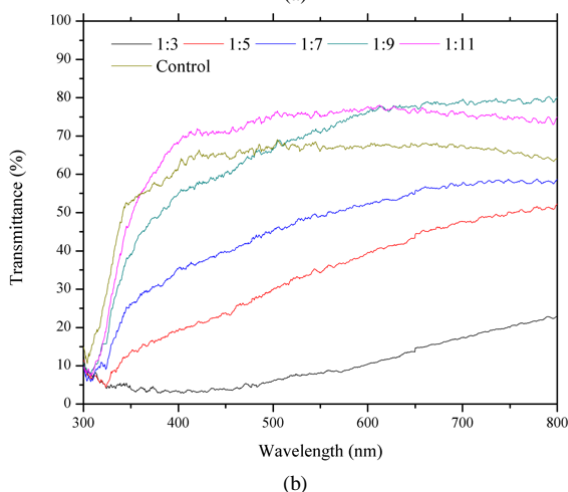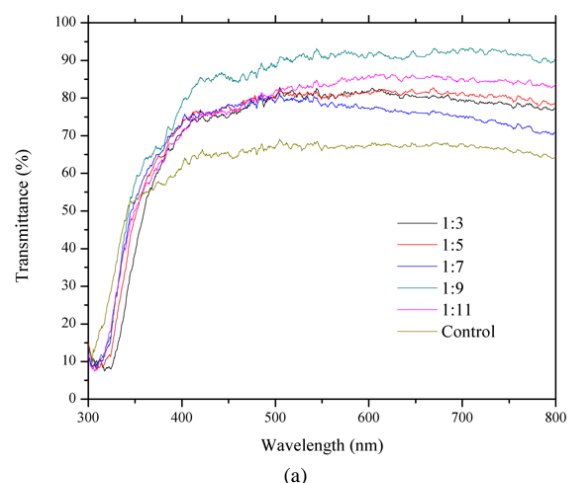

(a)

(b)

Figure 6. Ultraviolet-visible transmittance spectra of TiO_2 mesoporous electron transport layer with: (a) Transparent and (b) Opaque
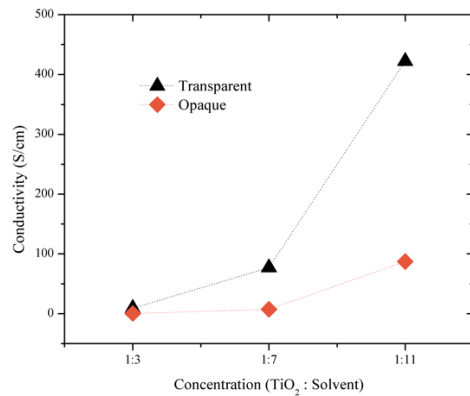
Figure 7. Electrical conductivity of TiO$_2$ mesoporous electron transport layer under different TiO$_2$ concentration

The electrical characteristic of a layer is one of the important factors for deciding whether a material is good for the electron transport layer. Ideally, the electron transport layer should have high conductivity, because it will increase the performance of charge accumulation and transfer process from the perovskite layer to electrode [3]. The electrical conductivity of the TiO$_2$ layer was obtained by measuring sheet resistance using a four-point probe equipped with an HP 3468A electrometer. The conductivity value is inversely proportional to the sheet resistivity value. Figure 7 shows the electrical conductivity of the TiO$_2$ layer at various concentrations. It was found that the electrical conductivity of the TiO$_2$ layer increases as TiO$_2$ concentration decreases, both opaque and transparent. The conductivity of the transparent layer is higher than the opaque layer. An opaque layer has a massive particle, which can be attributed to the high level of recombination and low electron density in the active layer [18].

Electrical performance of the fabricated perovskite solar cell with the configuration of FTO/CL- TiO$_2$/MS-TiO$_2$/Perovskite/ P3HT/Ag was presented in the current-voltage curve, as seen in Figure 8. In the transparent TiO$_2$ layer (Figure 8(a)), V$_{oc}$ increases from the ratio of 1:3 to 1:7. Later, it decreases from a ratio of 1:7 to 1:11. While on the opaque TiO$_2$ layer (Figure 8(b)), the change in V$_{oc}$ value is not significant. The voltage of the transparent TiO$_2$ layer increases from 0.07 V to 0.35 V, and the voltage of the opaque TiO$_2$ layer increases from 0.11 V to 0.18 V. While in the resulting of I$_{sc}$ value, the transparent TiO$_2$ layer is also higher than opaque TiO$_2$ layer. Sample with TiO$_2$ ratio of 1:7 has the high V$_{oc}$ and I$_{sc}$, both in the transparent and opaque TiO$_2$ layer.

The performance parameters of the devices can be calculated from the I-V curve in Figure 7, and the results are presented in Table 2. The performance parameter of the control (sample without TiO$_2$ electron transfer layer) is also presented in the table. From Table 2, we can see that sample "control" did not generate any current; meanwhile, the others did generate current with different values. This could be caused by the long travel distance electron must take before finally reach the electron transport layer to be transported to the FTO.
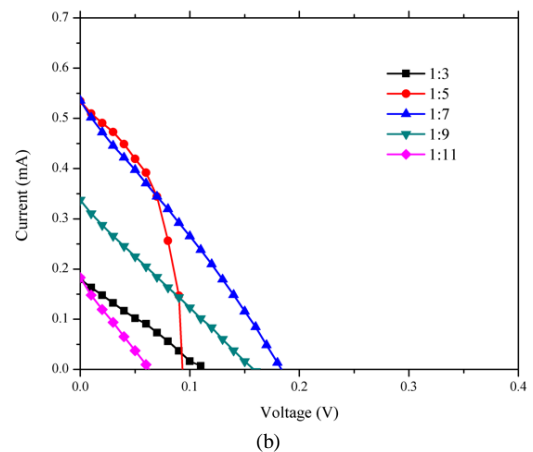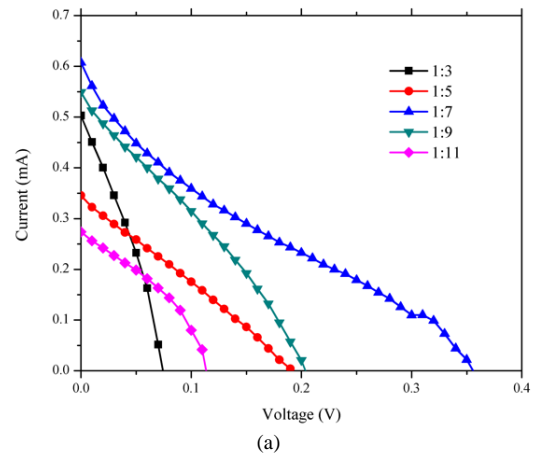

(a)

(b)

Figure 8. Current-voltage curves of perovskite solar cell with different TiO$_2$ concentration with: (a) Transparent, (b) Opaque.

With a mesoporous structure that acts as a scaffold for the perovskite layer, electron travel distance is significantly reduced and, in turn, reducing the possibility of recombination [10].

As seen in the I-V curve in Figure 7, the TiO$_2$ paste's ratio of 1:7 results in the highest V$_{oc}$ and I$_{sc}$, hence the resulting performance becomes the best. The power conversion efficiency (PCE) of the transparent TiO$_2$ layer and opaque TiO$_2$ layer is 0.37% and 0.21%, respectively. Thus, the best performance is obtained by a transparent TiO$_2$ layer.

TABLE 2
ELECTRICAL CHARACTERISTICS OF THE FABRICATED PEROVSKITE SOLAR CELL

Sample Name	V$_{oc}$ (V)	J$_{sc}$ (mA/cm²)	FF	PCE (%)
Control	Not generating any current			
1:3 T	0.07	2.01	0.28	0.09
1:5 T	0.19	1.38	0.15	0.14
1:7 T	0.35	2.43	0.19	0.37
1:9 T	0.20	2.19	0.27	0.26
1:11 T	0.11	1.09	0.33	0.09
1:3 AO	0.11	0.71	0.25	0.04
1:5 AO	0.07	2.04	0.28	0.11
1:7 AO	0.18	2.14	0.21	0.21
1:9 AO	0.17	1.34	0.18	0.10
1:11 AO	0.06	0.73	0.27	0.02

Overall, the resulting efficiency value is still very low compared to the perovskite solar cells in general, which is > 10% [10,13,19]. The resulting low efficiency is due to low V_{oc} and I_{sc} values. The V_{oc} value is determined by the difference between the LUMO electron transfer layer and the HOMO transfer hole layer on the perovskite solar cell work function diagram, as seen in Figure 1. The low V_{oc} value (< 0.35 V) in this study can be caused by changes in the work function of one or both of these layers. The work function of a material can change when there are additives added to the material intentionally or not [20]. In this study, silver was estimated to act as an impurity entering P_3HT semiconductor material, thereby increasing its conductive properties by changing its valence and conductive band values, which results in a reduced bandgap value. This short bandgap can cause a low V_{oc} value obtained. Silver also makes the resulting low I_{sc} values due to deeper penetration into the perovskite layer. In addition, optimization of the perovskite layer and hole P3HT HTM needs to be done further.

CONCLUSION

Perovskite solar cells have been fabricated with the configuration of FTO/CL-TiO$_2$/MS-TiO$_2$/Perovskite/P3HT/Ag. In order to optimize TiO$_2$ mesoporous as an electron transport layer, the concentration of transparent and opaque TiO$_2$ nanoparticles was varied. Results showed that transparent TiO$_2$ had a higher conductivity and transmittance compared to opaque. The concentration of the TiO$_2$ solution in a 1:17 ratio resulted in higher electrical performance in both transparent and opaque TiO$_2$ layers. The best perovskite solar cell's performance with PCE of 0.37% was achieved from the sample using a transparent TiO$_2$ layer with a concentration of 1:7 ratio.

ACKNOWLEDGMENT

REFERENCES

[1] X. Yang, H. Wang, B. Cai, Z. Yu, and L. Sun, "Progress in hole transporting materials in perovskite solar cells," *J. Energy Chem.*, vol. 27, pp. 650-672, May 2018.

[2] Y. Liu, Q. Chen, H. S. Duan, H. Zhou, Y. M. Yang, H. Chen, S. Luo, T. B. Song, L. Dou, Z. Hong, and Y. Yang, "A dopant-free organic hole transport material for efficient planar heterojunction perovskite solar cells," *J. Mater. Chem. A*, vol. 3, iss. 22, pp.11940-11947, Apr. 2015.

[3] T. B. Song, Q. Chen, H. Zhou, C. Jiang, H. H. Wang, Y. (Michael) Yang, Y. Liu, J. You, and Y. Yang, "Perovskite solar cells: film formation and properties," J. *Mater. Chem. A*, 3, Iss.17, pp. 9032-9050, Mar. 2015.

[4] E. S. Rosa, N. M. Nursam, Shobih, and R. Abdillah, "Improving the efficiency of perovskite solar cell through the addition of compact layer under TiO$_2$ electron transfer material," *Mater. Sci. Forum,* vol. 929, pp. 218-224, 2018.

[5] Z. Wan, M. Xu, Z. Fu, D. Li, A. Mei, Y. Hu, Y. Rong, H. Han, "Screen printing process control for coating high throughput titanium dioxide layers toward printable mesoscopic perovskite solar cells," *Front. Optoelectron.*, vol. 12, pp. 344-351, Apr. 2019.

[6] J. You, Y. (Michael) Yang, Z. Hong, T. B. Song, L. Meng, Y. Liu, C. Jiang, H. Zhou, W. H. Chang, G. Li, and Y. Yang, "Moisture assisted perovskite film growth for high performance solar cells," *Appl. Phys. Lett*., 105. 183902. 10.1063/1.4901510. 2014 vol. 105, pp. 183902.1-183902.5, 2014.

[7] Z. Xiao, C. Bi, Y. Shao, Q. Dong, Q. Wang, Y. Yuan, C. Wang, Y. Gao, and J. Huang, "Efficient, high yield perovskite photovoltaic devices grown by interdiffusion of solution-processed precursor stacking layers," *Energy Environ. Sci.*, vol. 7, iss. 8, pp. 2619-2623, May 2014.

[8] C. H. Chiang and C. G. Wu, "Bulk heterojunction perovskite–PCBM solar cells with high fill factor," *Nat. photonics*, vol. 10, pp. 196-201, Feb. 2016.

[9] P. W. Liang, C. Y. Liao, C. C. Chueh, F. Zuo, S. T. Williams, X. K. Xin, J. Lin, A. K.Y. Jen, "Additive enhanced crystallization of solution-processed perovskite for highly efficient planar-heterojunction solar cells," *Adv. Mater.*, vol. 26, iss. 22, pp. 3748-3754, Jun. 2014.

[10] J. You, L. Meng, T. B. Song, T. F. Guo, Y. (Michael) Yang, W. H. Chang, Z. Hong, H. Chen, H. Zhou, Q. Chen, Y. Liu, N. de Marco, and Y. Yang., "Improved air stability of perovskite solar cells via solution-processed metal oxide transport layers," *Nat. Nanotech.*, vol. 11, pp. 75-81, Jan. 2016.

[11] T. S. Su, T. Y. Hsieh, C. Hong, and T. C. Wei, "Electrodeposited ultrathin TiO$_2$ blocking layers for efficient perovskite solar cells," *Sci. Rep.*, vol. 5, pp. 16098.1-16098.8, Nov. 2015.

[12] S. Ito, "Sensitization and functions of porous titanium dioxide electrodes in dye-sensitized solar cells and organolead halide perovskite solar cells," in *Series on Chemistry, Energy, and Environment: Perovskite Solar Cells Principle, Materials and Devices*, vol. 1, E. W. G. Diau and P. C. Y. Chen, Ed. Singapore: World Scientific, 2017, pp. 45-61.

[13] G. Yang, H. Tao, P. Qin, W. Ke, and G. Fang, "Recent progress in electron transport layers for efficient perovskite solar cells," *J. Mater. Chem. A,* vol. 4, iss. 11, pp. 3970-3990, Jan. 2016.

[14] H. K. Park, D. K. Kim, and C. H. Kim, "Effect of dispersant on titania particle formation and morphology in thermal hydrolysis of TiCl$_4$," *J. Am. Ceram. Soc.*, vol. 80, iss. 3, pp. 743-749, Mar. 1997.

[15] S. Nakade, M. Matsuda, S. Kambe, Y. Saito, T. Kitamura, T. Sakata, Y. Wada, H. Mori, and S. Yanagida, "Dependence of TiO$_2$ nanoparticle preparation methods and annealing temperature on the efficiency of dye-sensitized solar cells," *J. Phys. Chem. B*, vol. 106, iss. 39, pp. 10004-10010, Oct. 2002.

[16] S. Ito, T. N. Murakami, S. M. Zakeeruddin, T. Yazawa, M. Mizuno, S. Kayama, and M. Greatzel, "Effects of TiO$_2$ particle size on the performance of dye-sensitized solar cells using ionic liquid electrolytes," *Nano*, vol. 9, no. 5, pp. 1440010.1-1440010.11, 2014.

[17] Z. Wan, M. Xu, Z. Fu, D. Li, A. Mei, Y. Hu, Y. Rong, and H. Han, "Screen printing process control for coating high throughput titanium dioxide layers toward printable mesoscopic perovskite solar cells," *Front. Optoelectron.*, vol. 12, pp. 344-351, Apr. 2019.

[18] H. Y. Yang, W. Y. Rho, S. K. Lee, S. H. Kim, and Y. B. Hahn, "TiO$_2$ nanoparticles/nanotubes for efficient light harvesting in perovskite solar cells," *Nanomater.*, vol. 9, iss. 3, pp. 326.1-326.10, Mar. 2019.

[19] K. Sveinbjornsson, K. Aitola, J. Zhang, M. B. Johansson, X. Zhang, J. P. C. Baena, A. Hagfeldt, G. Boschloo, and E. M. J. Johansson, "Ambient air-processed mixed-ion perovskites for high efficiency solar cells," *J. Mater. Chem. A*, vol. 4, iss. 42, pp. 16536-16545, Sep. 2016.

[20] A. Hagfeldt, G. Boschloo, L. Sun, L. Kloo, and H. Petterson, "Dye-sensitized solar cells," *Chem. Rev.*, vol. 110, no. 11, pp. 6595-6663, Sep. 2010.